JOURNAL OF MATERIALS SCIENCE 21 (1986) 3590–3600

Tension and flexural strength of silicon carbide fibre-reinforced glass ceramics

K. M. PREWO
United Technologies Research Center, East Hartford, Connecticut 06108, USA

The use of silicon carbide-type fibres to reinforce lithium aluminosilicate glass ceramics results in composites with exceptional levels of strength and toughness. It is demonstrated that composite strength and stress–strain behaviour depend on *in situ* fibre strength, matrix composition, test technique and atmosphere of test. Both linear and non-linear tensile stress–strain curves are obtained with ultimate strengths at 22° C approaching 700 MPa and failure strains of 1%. Flexure tests performed at up to 1000° C in air are compared with data obtained in argon to demonstrate a significant dependence of strength and failure mode on test atmosphere. Finally, glass ceramic matrix composite performance is compared with a silicon carbide fibre-reinforced epoxy system to demonstrate the importance of matrix failure strain on strength and stress–strain behaviour.

1. Introduction

The development of a silicon carbide-type fibre from an organometallic precursor [1] has led to a major resurgence of interest in fibre-reinforced ceramic matrix composites. By combining this high strength fibre with a variety of ceramic matrices it has been possible to achieve tough composites offering significant potential advantages over monolithic ceramics and carbon–carbon for high temperature applications. Composite fabrication approaches to create matrices around these fibres have included the densification of glasses and glass ceramics [2–4] and the chemical vapour infiltration of silicon carbide, [5]. Each of these composite fabrication approaches offers particular advantages and can provide materials with unique characteristics. The use of glass ceramics is viewed to be a particularly useful approach due to the wide range of matrix chemistries which can be created and the rapidity and ease with which composite articles can be fabricated.

The investigation described here was undertaken to develop a better understanding of the strength exhibited by the silicon carbide fibre-reinforced glass ceramic system using two different matrix chemistries, both based on lithium aluminosilicate (LAS). The general characteristics of one of these composites was reported previously [4]. Using a matrix which will be designated LAS-I in the following description, composite strength and toughness were reported at that time as a function of test temperature in an inert atmosphere. The reported properties were high enough to warrant the further assessment of composite performance described here as a function of matrix composition, test technique, test temperature and environment.

2. Experimental procedure

2.1. Composite fabrication

All composites were fabricated by hot press diffusion bonding. The reinforcing fibres were a silicon carbide type yarn (Nicalon fiber, Nippon Carbon Company). Fibre properties provided by the manufacturer indicated an average strength of 2480 to 3240 MPa and an average elastic modulus of 180 to 200 GPa. Two different glass ceramic matrices were used. Designated LAS-I and LAS-II, both of these matrices consist predominantly of standard lithium aluminosilicate (LAS) glass ceramic composition (Corning Code 9608). The deviations from the standard composition are that both matrices were tailored to be more compatible with the SiC-type fibres.

The overall fabrication process involves the following steps:

1. Make tape by infiltration of the SiC yarn with a glass powder slurry and controlled wrapping on to a mandrel. Dry and remove tape from the mandrel.
2. Cut tape into plys of desired size and fibre orientation and lay up composite.
3. Remove fugitive binder from tapes.
4. Hot press densify composite.
5. After removal from the hot press the composites can be heat treated (ceramed) or left in the as-pressed condition for final specimen machining.

In all cases flat plates were fabricated and specimens removed by using a diamond cutting wheel.

2.2. Mechanical testing

Because of a concern for relating composite performance to the fibre properties, individual fibres were tensile tested both before (as-received condition) and after composite fabrication (extracted). The as-received fibres were removed from the 500 fibre-containing tows by first burning off the sizing (vinyl acetate) in a bunsen burner flame while fibres were extracted from composites using hydrofluoric acid. Individual 7.5 cm lengths of individual fibres were then mounted on glass slides and then diameters measured at three locations each within the central

0022–2461/86 $03.00 + .12

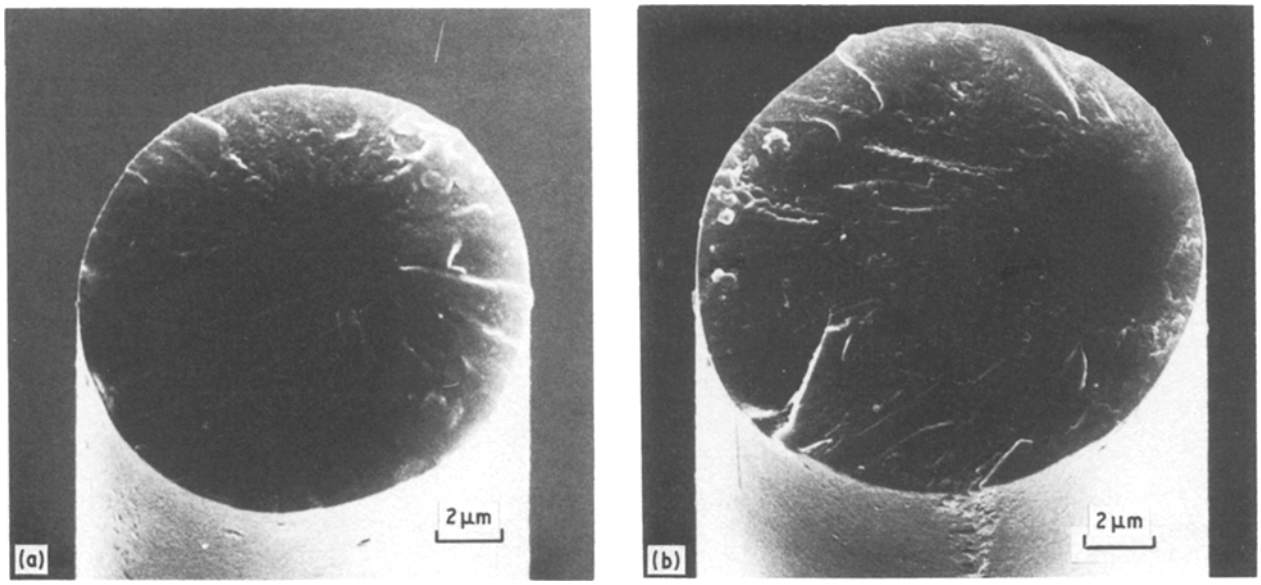

Figure 1 Fibre fracture surfaces. (a) High strength fibre 2780 MPa, (b) weak fibre 1760 MPa.

2.5 cm section. An average diameter was then taken for each individual fibre by averaging these values. The fibres were then carefully aligned and glued horizontally to the grips of a specially constructed fibre tensile test apparatus leaving a 2.5 cm gauge length. When fibre fracture surfaces were to be examined after test, the selected fibres were submerged in a drop of water which was held on a glass slide just below the gauge section. This water served to damp out the elastic shock waves on fracture, to minimize secondary fracture, and also retained fragments to help ensure the location of primary fracture. Individual fibre tensile strength was then calculated from the average fibre diameter and the maximum applied load at failure.

Composite tensile testing was performed using parallel-sided flat specimens on to which glass fibre-reinforced epoxy tabs were bonded. Overall specimen length was 10 cm, specimen width 1.0 cm, specimen thickness approximately 0.2 cm and the gauge length between doublers was maintained at 2.5 cm. Specimen strain was measured using strain gauges on both wide specimen faces.

Three- and four-point flexure tests were performed in both air and argon atmospheres up to a temperature of 1100° C. The crosshead rate of speed was maintained at 0.002 cm sec^{-1} for all tests; however, specimen span to depth ratios were varied to alter the state of applied stress. For the purposes of this paper, L represents the major test span, h the specimen depth (thickness), KL the distance between inner span and outer span loading points for four-point bend, P the applied load, σ_{max} the maximum outer surface flexural stress and τ_{max} the maximum shear stress at the specimen midplane. Thus, the ratio of applied maximum flexure to shear stresses was controlled by specimen and test fixture geometry according to the following two formulae

$$\frac{\sigma_{max}}{\tau_{max}} = \frac{2L}{h} \quad \text{for three-point bend} \quad (1)$$

$$\frac{\sigma_{max}}{\tau_{max}} = \frac{4KL}{h} \quad \text{for four-point bend} \quad (2)$$

These two equations are based on simple elastic beam theory and thus, as will be shown for the non-linear behaviour of some of the materials tested, are an oversimplification. However, they are useful to assess the relative magnitudes of the stresses applied during at least the initial elastic loading of the samples.

3. Experimental results and discussion

3.1. Fibre tensile test results

Individual fibres were tested in the as-received and extracted from composite conditions. In this way it was intended to be able to determine whether fibre performance can be related to measured composite strength. Several general observations can be made about these measurements.

1. The fibre diameters varied considerably from fibre to fibre within a given tow of fibres. However, the diameter of any given 2.5 cm central gauge length of fibre was nearly constant. At most, the variation in diameter was 10% and usually the variation was less than that. This provided confidence for the procedure of measuring fibre diameter before fibre test and not at the actual point of failure.

2. The majority of fractures occurred in the 2.5 cm gauge length. Those fractures which occurred at, or very near, the attached ends were also regarded as being valid test points.

3. It was possible to preserve some fibre fracture surfaces for scanning electron microscopic examination. In the case of weak fibres, the location of fracture was easily identified while for the strongest fibres multiple fractures frequently occurred. The use of the water drop to restrain fibre vibration and contain the fracture fragments was helpful to minimize this difficulty. The fracture surface morphology of strong and weak fibres is shown in Fig. 1. In some cases it was possible to locate probable centre-initiated origins of failure for strong fibre and surface-initiated for weak fibre. However, many fracture surfaces appeared rather indistinct and often it was not possible to determine a probable origin for failure.

A typical Weibull plot of the data obtained from a

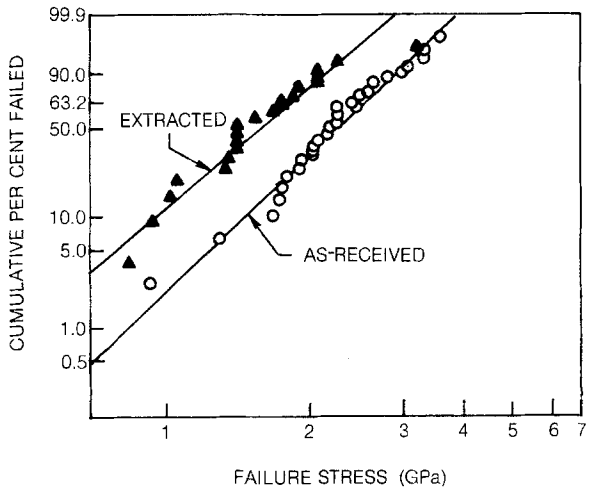

Figure 2 Two parameter Weibull plot of individual fibre tensile strengths.

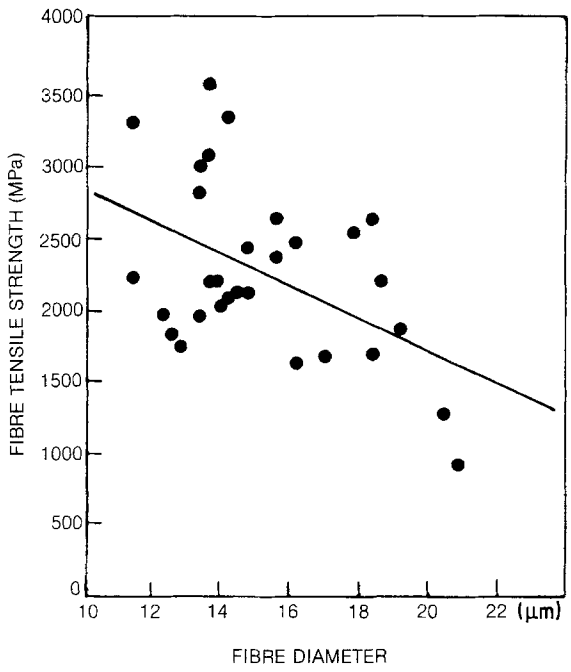

Figure 3 Dependence of individual fibre strength on diameter for as-received fibres.

spool of as-received and extracted SiC fibres is presented in Fig. 2. For the as-received fibre the individual fibre strengths varied from a low of 940 MPa to a high of 3665 MPa. The average ultimate strength for these data is 2300 MPa with a standard deviation of 620 MPa and a Weibull parameter of 4.2. An attempt was made to determine if fibre tensile strength could be related to the individual fibre diameters. (Fig. 3), and although a least square fit to the data does indicate a general increase in strength with decreasing diameter, the existence of a clear strength dependence was not shown.

An overall tabulation of as-received and extracted fibre stengths is presented in Table I. Included in the table are also overall average fibre diameters for each fibre spool. It can be seen that the as-received fibre strengths varied significantly among the spools tested and also that all of the fibres experienced a significant reduction in strength as a result of composite fabrication. Fibres extracted from composites having the LAS-I and LAS-II type matrices exhibited 40% and 30% strength losses, respectively. There was no additional strength loss associated with the ceramic heat-treatment process. The reasons for this strength reduction, which amounted to approximately 800 MPa for both matrix composites, was not determined; however, it was noted that the extracted fibres were more wavy after hot pressing and this can cause a strength reduction. The degree to which this is important is difficult to assess. To cause a 690 MPa reduction in average fibre strength, fibres of this diameter and elastic modulus would have to assume a bend having a radius of approximately 0.22 cm (using a fibre radius of 0.75×10^{-3} cm and elastic modulus of 192 MPa). In general the degree of waviness in these fibres was not this severe and other contributing factors must be sought. The induced waviness is created at the high temperatures of hot pressing since the fibres are forced into contact with their neighbours and do not lie perfectly parallel in the structure. Extensive deformation of these fibres at the temperatures of composite fabrication (above 1200° C) has been shown to occur [6] as has significant reduction in strength due to grain growth and the loss of excess carbon [7].

3.2. Composite 0° tensile strength and stress–strain behaviour

A series of unidirectionally reinforced composites was tested to determine levels of axial strength and relate strength to fibre and matrix properties. The composites were made with both LAS-I and LAS-II matrices.

TABLE I SiC fibre tensile test data

Fibre spool no.	Composite matrix	Fibre condition	No. fibres tested	Average diameter (μm)	Average UTS (MPa)	Standard deviation (MPa)	Weibull Parameter, *m*
967	–	As-received & cleaned	26	14	1820	560	3.6
	–	HF acid soaked	19	15	1810	630	3.2
	LAS-I	Extracted from composite 2160 (as-pressed)	20	16	1070	250	4.8
840	–	As-received & cleaned	19	15	2020	430	5.4
	LAS-I	Extracted from composite 2157-6 (ceramed)	20	14	1200	450	2.9
4585	–	As-received & cleaned	30	15	2300	610	4.2
	LAS-II	Extracted from composite 2369-7 (as-pressed)	20	17	1580	460	3.8
	LAS-II	Extracted from composite 2369-7c (as-pressed)	20	17	1520	600	2.7
	LAS-II	Extracted from composite 2376-2 (as-pressed)	20	15	1470	430	3.9
	LAS-II	Extracted from composite 2376-5c (ceramed)	20	15	1450	520	3.1

TABLE II 0° tensile test data for unidirectional SiC fibre reinforced LAS matrix composites

Comp. no.	Matrix	Matrix condition	Vol % fibre	Elastic modulus (GPa)	Tensile strength (MPa)	Failure strain, ε_f (%)	Prop. lim. stress (MPa)	Prop. lim. strain, ε (%)
2157-3C	LAS-I	Ceramed	46	–	485	–	–	–
-4C				132	429	0.32	–	–
-5C				134	451	0.34	–	–
				av. 133	455	0.33		
2369-4	LAS-II	As-pressed	46	–	758	–	–	–
-5				130	717	0.87	362	0.28
-6				138	785	1.06	400	0.29
				av. 134	758	0.97	381	0.28
-4c		Ceramed		130	681	0.88	429	0.33
-5c				124	641	0.78	424	0.34
				136	670	0.91	464	0.34
				av. 130	664	0.86	439	0.34
2376-5	LAS-II	As-pressed	44	–	673	–	–	–
-6				126	683	0.93	328	0.26
-7				130	653	0.87	363	0.28
				av. 128	670	0.90	345	0.27
2376-4c		Ceramed		140	686	0.88	367	0.26
-5c				133	664	1.08	398	0.30
-6c				136	686	1.03	410	0.30
				av. 136	680	1.03	391	0.29

The axial tensile stress–strain data obtained are listed in Table II where it can be seen that there is a significant difference in composite performance between LAS-I and LAS-II matrix systems. It is also important to note that the tensile strength of the LAS-II matrix composites can approach 750 MPa and their ultimate failure strain approaches 1%.

The tensile stress–strain curve for a ceramed 0°-SiC/LAS-I composite is shown in Fig. 4. The specimen exhibited perfectly linear stress-strain behaviour up to the point of fracture. In contrast, the tensile stress–strain behaviour of the 0°-SiC/LAS-II composites was markedly non-linear (Fig. 5). For both the as-pressed and ceramed conditions the curves exhibit a proportional limit at a strain of approximately 0.3%. The proportional limit is the point at which the stress–strain curve initially deviates from linearity. The exact levels of proportional limit stress and strain are listed in Table II showing that it generally occurs at a slightly higher stress and strain for the ceramed specimens. In contrast, no consistent difference in elastic modulus or final composite strength could be similarly noted.

The values of composite elastic moduli (E_c) reported in Table II can be compared with a simple rule of mixtures calculation based on both the advertised fibre elastic modulus (E_f) of 180 to 200 GPa and a standard ceramed LAS elastic modulus (E_m) of 86 GPa.

$$E_C = E_f V_f + E_m V_m \quad (3)$$

The anticipated composite modulus, for a 46 vol % fibre composite is then 130 to 138 GPa. This is in excellent agreement with the average values measured of 133 and 130 GPa (Table II) for the LAS-I and

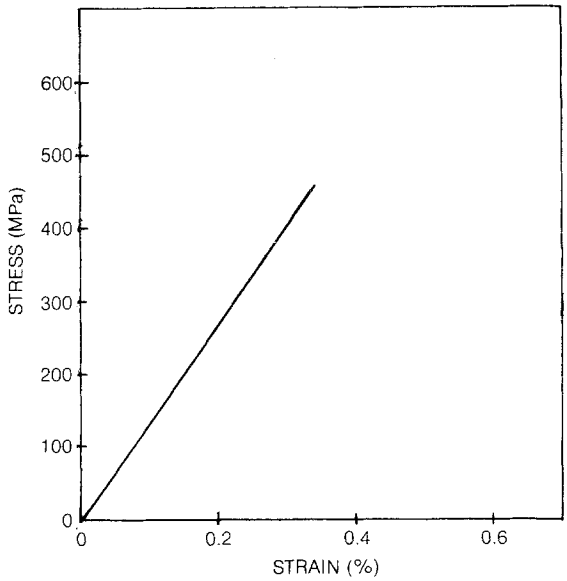

Figure 4 Tensile stress–strain curve for 0°-SiC fibre-reinforced LAS-I (ceramed) at 22° C.

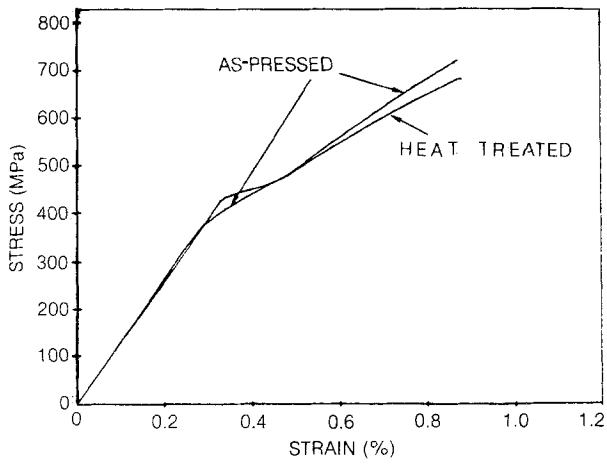

Figure 5 Tensile stress–strain curve for 0°-SiC fibre-reinforced LAS-II in the as-pressed and ceramed conditions at 22° C.

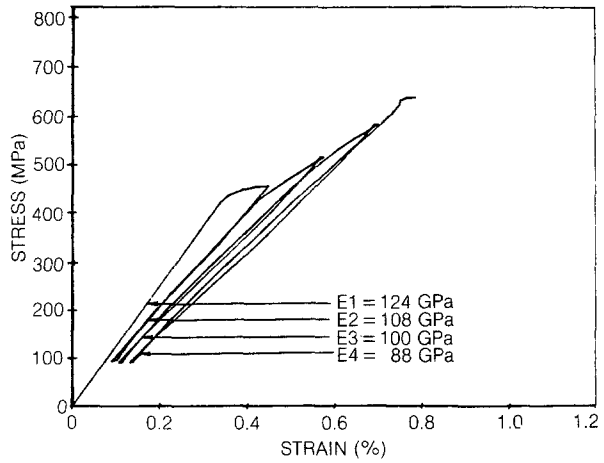

Figure 6 Cycled tensile stress–strain curves for 0°-SiC reinforced LAS-II (ceramed) at 22° C.

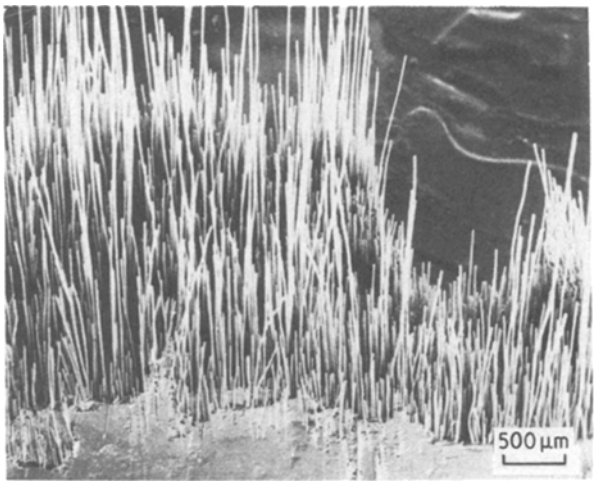

Figure 7 Tensile fracture surface 0°-SiC fibre-reinforced LAS-II (as-pressed) tested at 22° C.

LAS-II matrix composites, respectively, containing 46 vol % fibre.

If the existence of the proportional limit in the LAS-II matrix composite stress–strain behaviour is associated with matrix cracking taking place, it may be assumed that the composite elastic modulus will decrease when strained beyond this limit. The data in Fig. 6 would seem to confirm this. The stress–strain curve in this figure was obtained by loading and unloading several times as shown. The elastic modulus of the composite decreases substantially with increasing strain and, as shown in the figure, a modulus 30% less than the initial composite elastic modulus can be achieved at a strain approaching the ultimate fracture strain. It is also important to note that this specimen was not degraded in its ultimate strength when compared to uncycled composites.

The fracture surfaces of both the LAS-I and LAS-II matrix composites generally exhibited extensive fibre pull-out (Fig. 7). No difference could be discerned between the appearance of as-pressed and ceramed specimens and higher magnification examination of the pulled out fibres clearly demonstrated that they are pulled out cleanly from the surrounding matrix.

Since fibres were extracted from specimens cut from the same composite panels that the tensile specimens were cut from, it was possible to compare fibre strength with composite strength. This is shown in Table III using three different predictive methods, all of which assume that the matrix itself provides absolutely no increment of strength at the point of composite failure. At the failure strains measured, which are in excess of 0.3%, this is probably a reasonable assumption.

Referring to the Table III column $S_A V_f$ simply takes the average extracted fibre strength (S_A) and multiplies it by the specimen fibre content, V_f. Used frequently in "rule of mixtures" calculations the use of this equation is mechanistically unsatisfactory in that it completely neglects the fibre strength distribution and hence the sequence and manner in which fibres fail. Nevertheless, this simple expression provides particularly good agreement with the measured composite strengths.

The $S_B V_f$ column in Table III uses a calculated value of fibre bundle strength, S_B, that takes into account fibre strength distribution [8]. The fibres are all assumed to act completely independently of each other and fail in sequence, beginning at the weakest. As each succeeding fibre fails all of the remaining fibres share the increased load increment released by the broken fibre. At the bundle strength, S_B, which is calculated based on the original area of all fibres, the remaining intact fibres are overloaded and fail at once. Because of the rather low Weibull parameter (m) values, the fibres tested exhibited a rather broad distribution in strength and hence also rather low bundle strengths. The m values used to calculate bundle strength are shown also in the table and the fibre bundle has the same gauge length as the individually tested fibres, 2.5 cm.

The $S_c V_f$ data (Table III) refer to an assumed cumulative fibre failure induced composite fracture. Introduced by Zweben and Rosen [9], this strength calculation is based on the assumption that, unlike in the above bundle model, breaking fibres transfer their load to their neighbours in a more complex manner. Upon fracture the matrix strains in the region of the

TABLE III 0° tensile strength of unidirectional composites

Composite	Matrix	Matrix condition	V_f* (%)	Measured composite av. tensile strength (MPa)	Predicted av. composite tensile strength					
					$S_A V_f$ (MPa)	m	$S_B V_f$ (MPa)	$S_c V_f$ (MPa)		
								L_c = 0.5 cm	L_c = 0.25 cm	L_c = 0.13 cm
2157	LAS-I	Ceramed	46	455	550	3	300	515	650	825
2369	LAS-II	As-pressed	46	758	730	4	440	660	790	925
		Ceramed		664	695	3	380	650	825	1050
2376	LAS-II	As-pressed	44	670	648	4	380	580	695	815
		Ceramed		680	634	3	340	590	745	940

TABLE IV 0° four-point flexure* data for unidirectional SiC fibre-reinforced LAS matrix composites

Comp. no.	Matrix	Matrix condition	Av. elastic modulus (GPa)	Failure mode†	Av. flexural strength (MPa)
2157	LAS-I	As-pressed	–	T	755
		Ceramed	138	T	758
2369	LAS-II	As-pressed	168	T + C	1370
		Ceramed	132	C	923
2376	LAS-II	As-pressed	172	T + C	1380
		Ceramed	161	C	1050

*$4K(L/h)$ = 58 to 35.
†T = tension, C = compression.

break are non-uniform and load cannot be transferred to a neighbour over some ineffective length L_c. In the case of the present composites the fibre–matrix bond strength is very low and, in fact, on fibre fracture debonding may occur. Composite failure occurs when a sufficient number of breaks occur in a given section of composite to achieve an overload failure, such as in the case of the bundle model above. But, since L_c is much less than L, the composite specimen gauge length, the composite strength can exceed strength S_B and the cumulative strength, S_C, depends on L, L_c and the Weibull parameter, m, in the following manner.

$$\frac{S_C}{S_B} = \left(\frac{L}{L_c}\right)^{1/m} \quad (4)$$

The values of $S_C V_f$ representing composite strength based on this model are shown in Table III for three different ineffective lengths, 0.5, 0.25 and 0.13 cm. The composite gauge length is 2.5 cm. Best agreement with measured composite strength would appear to be for some ineffective length of 0.5 to 0.25 cm which is in the range of fibre pull-out lengths observed for these composites.

As a final note, all of the above calculations assume that load transfer does not occur to a greater degree from one fibre directly to a nearest neighbour. This is highly unlikely. Thus, for shorter ineffective length materials the ability to form critical damage zones from which unstable crack growth can proceed will significantly diminish the composite strength and leave the above value of $S_c V_f$ as the upper bound strength.

3.3. Room-temperature composite flexure strength

While flexural tests are generally more easily performed than tensile tests, the interpretation of the resulting data can be much more difficult due to the potential for a wide range of failure modes. An example of this will be described here where a change from tension to compression failure leads to a major change in calculated flexural strength.

3.3.1. 0° flexure of LAS-I matrix composites

Specimens taken from the same composite panel as the LAS-I tensile specimens described above were tested in four-point flexure. The data, reported in Table IV, indicate no difference between as-pressed and ceramed composite flexural strength or failure mode. All specimens failed by forming cracks on the tensile side of the test specimens. By placing strain gauges on the front and back sides of two specimens it was possible to determine that the tension and compression stress-strain curves were nearly identical. Also of note is the observation that composite average flexural strength of 758 MPa is 1.67 times the composite tensile strength described in the last section.

To obtain a measure of composite variability, two unidirectionally reinforced composite panels were each cut into eleven flexure specimens and tested in three-point bend using a span-to-depth ratio of 25. Both panels were fabricated using the same spool of fibre and similar processing conditions which resulted in composites having a nominal fibre content of 50% by volume. The resultant values of composite flexural strength and elastic modulus are reported in Table V where the elastic modulus was calculated from specimen mid-span deflection against applied load curves. All of these specimens failed first by tensile cracks on their tensile sides and resisted complete fracture through diversion of the cracks such that they retained a major portion of their strength after test. When later broken by hand the specimens exhibited a fibrous fracture mode. It can be seen that there is a considerable difference in strength between panels and that the two populations do not overlap. Fibres were not extracted from the panels to determine whether this variation can be associated with fibre strength.

3.3.2. 0° flexure of LAS-II matrix composites

In contrast to the above composites, the LAS-II matrix system exhibited a marked difference in composite strength between as pressed and ceramed specimens (Table IV). The as-pressed specimens were significantly stronger, 1380 MPa, and exhibited a strength 1.8 to 2.1 times their previously described tensile strength. The reason for the major drop in ceramed composite flexural strength could not be attributed to a change in tensile strength; this had been shown not to depend on matrix condition (Table III). By examination of the flexure specimens during and after test, however, it was possible to find the reason

TABLE V Three-point flexural test data for 0°-SiC/LAS-I composite, for three-point bend $2L/n$ = 50

	Composite 2120 (11 specimens tested)		Composite 2119 (11 specimens tested)	
	Elastic modulus (GPa)	Flexural strength (MPa)	Elastic modulus (GPa)	Flexural strength (MPa)
Range	123–130	480–614	122–138	414–450
Average	127	552	130	430
Standard deviation	2.7	50	4.3	14.0
Weibull parameter	60	13.5	38	38

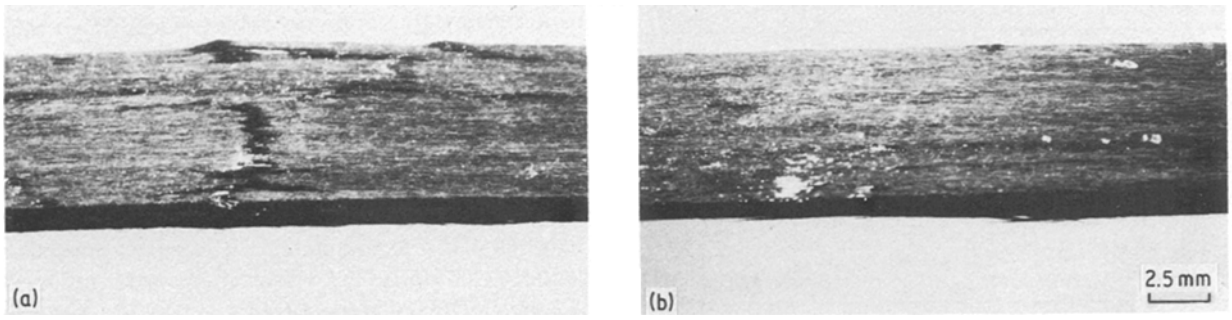

Figure 8 Tension surfaces of failed four-point bend specimens of 0°-SiC fibre-reinforced LAS-II. (a) As-pressed condition, (b) ceramed condition.

for the 25 to 30% drop in flexural load-carrying capability. In the as-pressed condition the specimens failed in tension, while in the ceramed case they failed in compression. The tension surfaces are shown in Fig. 8.

3.3.3. 90° flexure and thermal expansion of LAS-II matrix composites

In an attempt to understand further the difference between the as-pressed and ceramed LAS-II matrix composite, 90° flexural specimens were tested in four-point bend with strain gauges on the tension side only. The stress–strain curves in both the as-pressed and ceramed conditions were perfectly linear to failure and both the strength and elastic modulus were strongly dependent on matrix condition (Table VI). The lower 90° strength in the ceramed condition could be a major contributing factor to the lower ceramed composite 0° flexural strengths. Resistance to fibres buckling on the compression side of the four-point 0° flexure specimens is decreased by lower matrix constraint of the fibres.

Composite thermal expansion was measured in the 0° direction. Attempts to measure 90° specimens in the ceramed condition were felt unreliable due to the presence of cracks which yielded inconsistent curves. The 0° specimen data, shown in Fig. 9, indicate that the ceramed composite has a lower coefficient of thermal expansion (CTE), particularly at temperatures above 300° C. This change in CTE, as well as any matrix volume changes during ceraming, can contribute to matrix weakening in the composite by the creation of microcracks and in turn, decrease composite 0° compression strength.

TABLE VI 90° four-point flexure data for unidirectional SiC reinforced LAS-II matrix composites

Matrix condition	Elastic modulus (GPa)	Flexural strength (MPa)	ε_f (%)
As-pressed	85.4	23.4	0.03
	85.4	16.5	0.02
	78.0	20.7	0.03
Ceramed	42.0	12.4	0.03
	44.0	10.3	0.03
	36.5	11.0	0.04

3.4. Elevated temperature flexural strength

Both LAS-I and LAS-II matrix composites were tested in three- and four-point flexure up to a temperature of 1100° C. Because of a concern for the effects of atmosphere, tests were performed in air and an inert atmosphere of argon.

3.4.1. LAS-I matrix composites

The dependence of composite four-point flexural strength and stiffness on test temperature in air is shown in Fig. 10 where it can be seen that composite flexural strength increases with temperature up to 1100° C. The tests, also indicate a major decrease in composite stiffness, measured by the load against mid-span deflection traces. This was accompanied with a more noticeable rounding of the load–deflection curves with increasing temperature and at 1100° C a definite permanent bowing of the sample after test. Despite this stiffness decrease, which in part can be associated with matrix softening, the composite load-bearing capability increased with temperature. All of the specimens indicated that first failure occurred in the tension surface; however, when the specimens were subsequently broken apart by hand, there was a noticeable change in fracture surface morphology. At room temperature the fracture surfaces were very fibrous in appearance while at 600° C and above they were more "woody". This term will be illustrated in greater detail later; however, it refers to a jagged

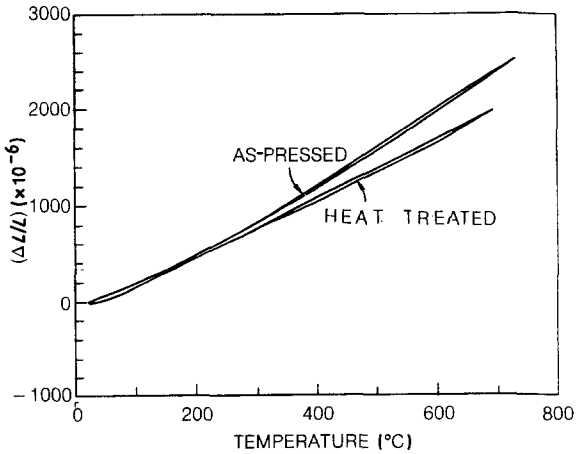

Figure 9 Thermal expansion of 0°-SiC fibre reinforced LAS-II. As-pressed condition CTE = $3.6 \times 10^{-6} C^{-1}$, ceramed condition CTE = $2.85 \times 10^{-6} C^{-1}$.

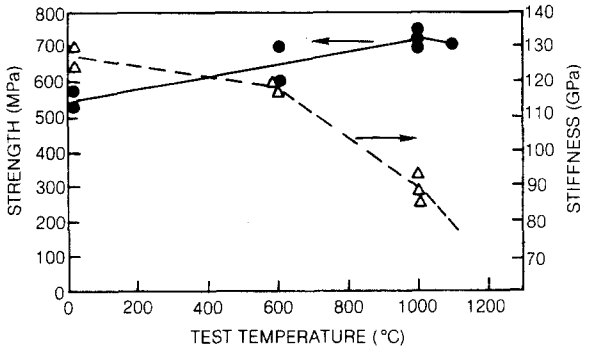

Figure 10 Four-point flexural strength and elastic modulus of 0°-SiC fibre-reinforced LAS-I (ceramed) tested in air. $4K(L/h) = 47$.

fracture that is made up of matrix plus fibre protrusions and not just individual fibres. These results differ somewhat from the data obtained by flexure testing in argon and reported previously for this same LAS-I matrix composite [4]. In the argon atmosphere, flexural strength also increased with increasing test temperature; however, the composite fracture surface remained extremely fibrous over the entire temperature range of test.

The above four-point bend tests were performed with a major span to specimen depth ratio such that the ratio of maximum applied flexural stress to shear stress was 47 which resulted in all specimens failing first in tension. To assess composite shear strength, thicker specimens were tested in three-point bend with a span-to-depth ratio of 5 creating a ratio of maximum applied flexural stress to shear stress of only 10. Unfortunately, at the time of test a suitable bend fixture was only available for use in inert atmosphere and hence these tests were performed in argon. Composite strength was taken from the maximum load achieved in each test and calculated in terms of both the maximum shear and flexural stresses achieved during test (Fig. 11). All of the initial load–deflection curves were linear up to the point of failure for the tests run between 22 and 1000° C. Only at 1100° C did the loading curves indicate any non-linear deformation prior to maximum load. In all cases the specimens once more did not suddenly fracture, but instead, decreased gradually in load-carrying capability with increasing deflection. At 22 and 600° C it was not possible to determine the origin of failure so it was not possible to say whether the specimens failed in shear, tension or compression. At 1000° C the specimens clearly failed on the tension surface, while at 1100° C they definitely failed by interlaminar shear. In the case of composite strength at the lower temperatures it can only be assumed that composite shear strength is either equal to, or greater than, the values shown. The room-temperature interlaminar shear strength value of 34.4 MPa for LAS-I matrix composites, however, is consistent with off-axis tensile data reported elsewhere [10].

3.4.2. LAS-II matrix composites

In contrast to the LAS-I matrix composites, the flexural strength of the LAS-II matrix system decreased dramatically at elevated temperature (Fig. 12). The data in the figure were obtained by three-point bend testing in air and similar results were also noted in four-point bend test. The decrease in composite strength was first noted at a test temperature of 700° C, however, even at 600° C it appeared that the fracture mode had changed from the fibrous type, typical of room temperature fractures, to a "woody" appearance. At the higher temperatures, however, the tensile sides of the flexure samples took on a notably flat fracture morphology. It should also be noted that at 600° C and above the primary fracture mode occurred on the tensile side of the specimens while at lower temperatures the fracture mode was compression, in agreement with the flexure test fracture mode described previously in this paper for fully ceramed LAS-II composites.

Fig. 13 illustrates the fracture surface of a three-point bend specimen tested in air at 900° C. The very flat side of the specimen was the side in tension where the tensile stresses in the presence of air cause a major embrittlement of the fracture process while compressive stresses do not. In the case of this particular specimen, the transition between brittle and fibrous fracture was extremely abrupt and occurred near the specimen centre thus corresponding roughly with the neutral axis, i.e. transition between tensile and compressive stresses. Fracture beyond this point of transition was not continued during test since the load was removed from the specimens after the first sign of

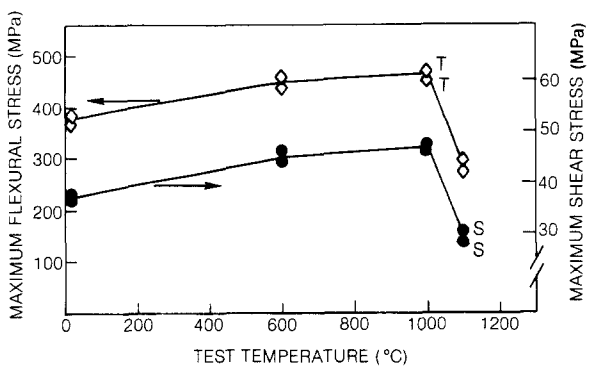

Figure 11 Calculated maximum shear and flexural stresses achieved in three-point bend for 0°-SiC fibre-reinforced LAS-I tested in argon. (T) denotes tensile failure and (S) denotes shear failure. $2(L/h) = 10$.

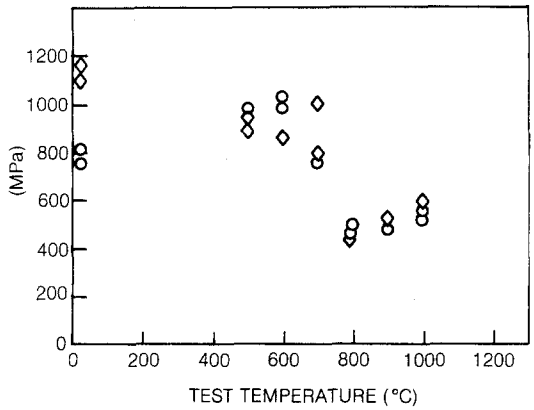

Figure 12 Three-point flexural strength of 0°-SiC fibre-reinforced LAS-II (ceramed) tested in air. (○) composite 2532, (◇) composite 2531. $2(L/h) = 50$.

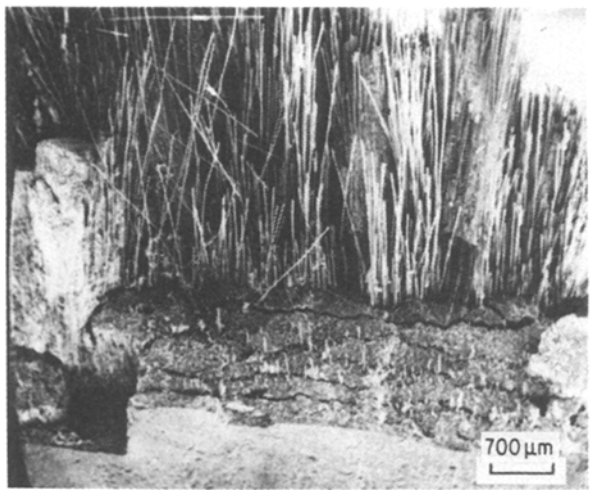

Figure 13 Fracture surface of a 0°-SiC fibre-reinforced LAS-II (ceramed) tested in three-point flexure in air at 900° C. The flat fracture region is closest to the tensile side.

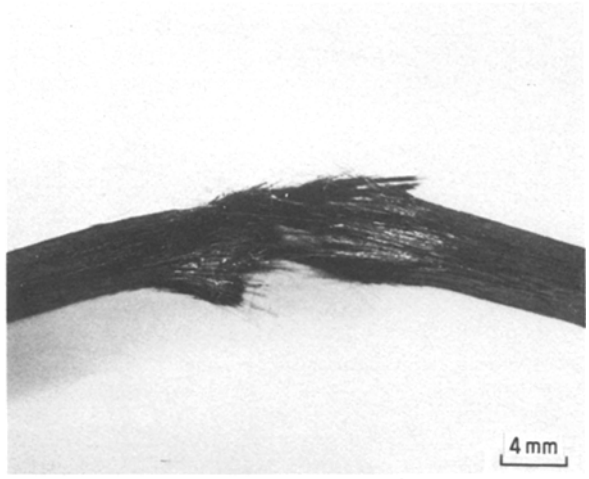

Figure 15 Four-point bend specimen of 0°-SiC/LAS-II after testing at 900° C in argon. Flexural strength = 1180 MPa.

fracture. The final fracture, to reveal the nature of the fracture surface itself, was performed by hand at room temperature.

Closer examination of the tensile side revealed two distinct features; flat regions normal to the applied stress and cracks which run predominantly prallel to the specimen tensile surface (Fig. 14). In the case of the flat regions, the fibres generally fracture within a distance less than their own diameter from the matrix surface while at the large crack boundaries the fibres were able to pull out at greater length due to their release from the matrix.

A further examination of the effects of test atmosphere was performed by testing several additional specimens in argon and comparing with specimens from the same composite plate tested in air. In each case the argon test atmosphere resulted in much higher strengths. A typical comparison is made in Figs 15 and 16 for specimens tested at 900° C in four-point flexure. In argon a strength of 1180 MPa was achieved, while in air the strength was reduced to 275 MPa. In this particular comparison the specimen tested in air exhibited the "woody" type of fracture morphology mentioned above. While this specimen did splinter into segments on the tension side, these segments did not exhibit fibres pulled out of the matrix, rather they remained bound into the matrix. The specimen tested in argon, in contrast, exhibited extension fibre pull-out from the matrix.

4. Conclusion

The axial strength of Nicalon fibre-reinforced glass ceramic matrix composites has been shown to be a function of a wide range of parameters. *In situ* fibre strength, matrix composition, test temperature and environment, and test technique have all been shown to play important roles. A comparison between the LAS-I and LAS-II matrix systems has shown that, even in simple tension, composite strength and stress–strain behaviour characteristics are significantly different. In large measure this was determined to be due to the difference in *in situ* fibre strength. Fibres extracted from the LAS-II matrix composites were stronger in approximately the same ratio as the relative composite strengths. A signficant difference in as-received fibre spool strengths, however, was more responsible for this difference in than any differences in fibre degradation during composite fabrication

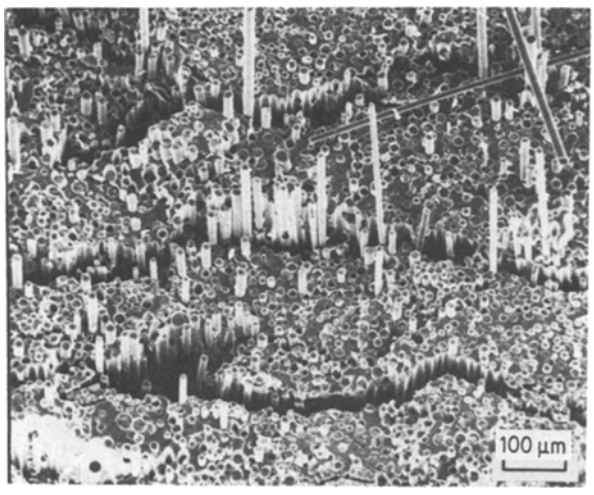

Figure 14 Higher magnification view of flat fracture region in Fig. 13, showing the limited degree of fibre pull-out and cracks running parallel to the fibre direction.

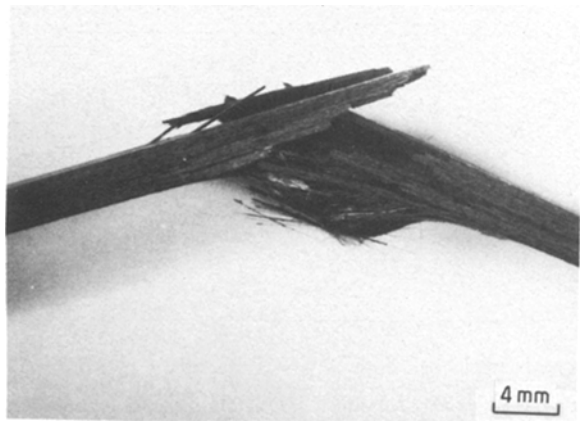

Figure 16 Four-point bend specimen of 0°-SiC/LAS-II after testing at 900° C in air. Flexural strength = 275 MPa.

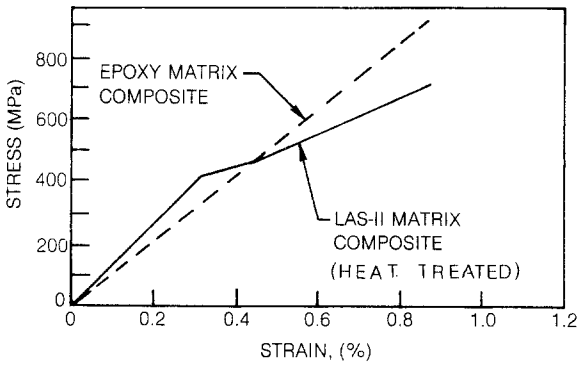

Figure 17 Tensile stress–strain comparison for 0°-SiC fibre-reinforced composites.

The higher fibre strength in the LAS-II composites also caused an increase in composite failure strain that far exceeded the increase in strength. This was due to the significant non-linear shape of the LAS-II composite tensile stress–strain curves. At a tensile strain of approximately 0.3% the slope of the stress–strain curve decreased significantly and was accompanied by a decrease in true elastic modulus, as determined by unloading and reloading the specimens several times. This behaviour can most probably be attributed to the occurrence of matrix microcracking [11, 12] and distinguishes the behaviour of ceramic matrix composites from that of their resin matrix counterparts. The comparison of composite tensile stress–strain curves in Fig. 17 demonstrates this point. Both composites are fabricated using Nicalon fibre; however, the epoxy matrix composite behaviour is perfectly linear to the point of fracture since the epoxy matrix failure strain is greater than that of the Nicalon fibres [13]. In addition, epoxy matrix composite tensile strength is greater, undoubtedly due to a superior retention of the micalon fibre strength during composite processing.

The existence of glass ceramic matrix microcracking prior to composite failure causes the composite elastic modulus to decrease with increasing tensile strain. This may prove to be a help in increasing composite toughness since, in the presence of a stress concentrator, local stresses will be reduced due to the increased compliance of the composite. It should be pointed out, however, that this non-linear stress–strain behaviour is not necessary to provide composite toughness since even the LAS-I matrix composites exhibited very fibrous fracture surfaces and have been shown to resist crack growth [4].

It has also been shown that composite flexural strength is not always a good indicator of composite tensile strength. In both the resin and glass ceramic matrix composite systems the flexural strength was considerably greater than the tensile strength (Table VII). However, as noted in this paper, the magnitude of this superiority depended on the fracture mode. An additional interesting comparison can be made between the epoxy matrix composite system and the LAS-II matrix composite in the as-pressed condition (Table VII). In pure tension the epoxy matrix composite exhibited a nearly 30% greater tensile strength than the LAS-II matrix composite, however, in flexure the ranking was reversed and the glass ceramic matrix composite was 10% greater in strength. This superiority in flexure is due to both the non-linear tensile stress–strain behaviour and also the high compression strength of the as-pressed LAS-II matrix system. The calculated maximum flexural stress for this material is not valid due to this non-linear tensile behaviour, which causes the neutral axis of stress to be displaced toward the compression side of the specimen with increasing applied load. The simple elastic calculations used to derive the composite flexural strength do not take this into account; however, the point that remains true is that the glass ceramic matrix composite beam was able to carry a significantly higher load than its epoxy matrix counterpart. This points to the unique advantage provided by the low matrix failure strain which permits the composite to "yield" prior to fracture.

Another important difference between epoxy and glass ceramic matrix composites can be found in the values of interlaminar shear strength. It is much higher for the epoxy matrix system (Table VII). While high interlaminar shear strengths are desired for epoxy matrix composites, the same cannot be said for glass ceramic matrix systems since the achievement of crack growth resistance is through low fibre–matrix interfacial strength and this provides a low strength shear path.

The matrix-dependent variation in composite strength retention with increasing test temperature in air can be related to the difference in composite stress–strain behaviour and may help explain the mechanism of degradation. The LAS-II matrix system relies on the ability to strain beyond the point of matrix microcracking to achieve high strength and hence, during testing, permits the surrounding test

TABLE VII Comparison of SiC fibre-reinforced epoxy and glass ceramic matrix composite properties

	Matrix				
	Epoxy*	LAS-I	LAS-I	LAS-II	LAS-II
Matrix condition	–	as-pressed	ceramed	as-pressed	ceramed
Fibre content (vol %)	–	46	46	44	44
Tension properties					
Strength (MPa)	875	–	455	670	680
Elastic modulus (GPa)	106	–	133	128	136
Failure strain (%)	0.84	–	0.33	0.90	1.03
Flexural strength (MPa)	1240	755	758	1380	1050
Ratio of flexural strength to tensile strength	1.42		1.67	2.06	1.54
Interlaminar shear strength (MPa)	87	–	34.4	–	–

*Epoxy matrix composite data from [13].

atmosphere to enter the composite structure. While testing in argon appears to be of no consequence, the entry of air into the structure causes a dramatic change in fracture mode. In air, fibre pull-out from the surrounding matrix is prevented either through a sudden local decrease in fibre strength or through an increase in fibre–matrix interfacial strength. In either event, this effect is not as important for LAS-I matrix composites since composite strength is much less to begin with and fracture even at room temperature occurs prior to extensive matrix microcracking.

It can be concluded that the Nicalon fibre-reinforced glass ceramic composite system provides two interesting composites for further investigation. Differing significantly in their stress–strain behaviour and high temperature strength characteristics they are both examples of crack growth-resistant ceramic composites that can be utilized as candidates for experimental investigations to ascertain which features of composite behaviour are of greatest significance and can also be used in selected applications to provide reliable, fracture tough, non-metallic materials.

Acknowledgements

The author would like to acknowledge the support of Drs A. Dines, R. Pohanka, S. Fishman and D. Siegel of the Office of Naval Research for the performance of this work and ONR funding under contract N00014-81-C-0571. In addition, the author is thankful for the help of his co-workers, Drs J. Brennan, G. Layden and Mr B. Jacob, The creation and supply of glass ceramic matrices through the co-operation of Drs K. Chyung and M. Taylor of Corning Glass is also greatly appreciated.

References

1. S. YAJIMA, K. OKAMURA, J. HAYASHI and M. OMORI, *J. Amer. Ceram. Soc.* **59** (1976) 324.
2. K. M. PREWO and J. J. BRENNAN, *J. Mater. Sci.* **15** (1980) 463.
3. *Idem, ibid.* **17** (1982) 1201.
4. J. J. BRENNAN and K. M. PREWO, *ibid.* **17** (1982) 2371.
5. M. DAUCHIER, P. LAMICQ and J. MACE, *Rev. Int. Hautes Temp. Refract.* **19** (1982) 285.
6. G. SIMON and A. R. BUNSELL, *J. Mater. Sci. Lett.* **2** (1983) 80.
7. T. MAH, N. L. HECHT, D. E. McMULLEN, J. R. HOENIGMAN, H. M. KIM, A. P. KATZ and H. A. LIPSITT, *J. Mater. Sci.* **19** (1984) 1191.
8. C. ZWEBEN, *Amer. Inst. Aeronautics Astronautics J.* **6** (1968) 2325.
9. C. ZWEBEN and B. W. ROSEN, *J. Mech. Phys. Solids* **18** (1970) 189.
10. K. M. PREWO, "Advanced Characterization of SiC Fiber Reinforced Glass Ceramic Matrix Composites", Office of Naval Research Contract N00014-81-C-0571, Interim Report, June 1983.
11. J. AVESTON, G. A. COOPER and A. KELLY, in Conference Proceedings National Physical Laboratory, "Properties of Fibre Composites" (IPC Surrey, 1971) pp. 15–26.
12. J. AVESTON and A. KELLY, *J. Mater. Sci.* **8** (1973) 352.
13. J. R. STRIFE and K. M. PREWO, *ibid.* **17** (1982) 65.

Received 5 November
and accepted 20 December 1985